

In the search for the low-complexity sequences in prokaryotic and eukaryotic genomes: how to derive a coherent picture from global and local entropy measures

Claudia Acquisti¹, Paolo Allegrini², Patrizia Bogani¹, Marcello Buiatti¹,

Elena Catanese³, Leone Fronzoni^{4,5}, Paolo Grigolini^{4,6,7}, Giuseppe Mersi¹, Luigi Palatella⁴

¹*Dipartimento di Biologia Animale e Genetica dell'Università degli Studi di Firenze, Via Romana 17, 50125 Firenze, Italy*

²*Istituto di Linguistica Computazionale del Consiglio Nazionale delle Ricerche,
Area della Ricerca di Pisa, Via Moruzzi 1, San Cataldo 56010 Ghezzano-Pisa, Italy*

³*Scuola Normale Superiore, Piazza dei Cavalieri, 56125 Pisa, Italy*

³*Dipartimento di Fisica dell'Università di Pisa and INFN, via Buonarroti 2, 56127 Pisa, Italy*

⁴*Centro Interdipartimentale per lo Studio dei Sistemi Complessi, via S. Maria 28, 56126 Pisa, Italy*

⁵*Center for Nonlinear Science, University of North Texas,
P.O. Box 311427, Denton, Texas 76203-1427 and*

⁶*Istituto dei Processi Chimico Fisici del CNR Area della Ricerca di Pisa, Via G. Moruzzi 1, 56124 Pisa, Italy*

We investigate on a possible way to connect the presence of Low-Complexity Sequences (LCS) in DNA genomes and the nonstationary properties of base correlations. Under the hypothesis that these variations signal a change in the DNA function, we use a new technique, called Non-Stationarity Entropic Index (NSEI) method, and we prove that this technique is an efficient way to detect functional changes with respect to a random baseline. The remarkable aspect is that NSEI does not imply any training data or fitting parameter, the only arbitrariness being the choice of a marker in the sequence. We make this choice on the basis of biological information about LCS distributions in genomes. We show that there exists a correlation between changing the amount in LCS and the ratio of long- to short-range correlation.

I. INTRODUCTION

In the recent past there has been a significant interest in the search for both long- and short-range correlation in DNA sequences [1, 2, 3]), The main results of these papers have been that the amount of long-range correlation increases when moving from prokaryotes to eukaryotes and from coding to non-coding sequences. This paper is devoted to discussing the same issue using two new theoretical tools that were not yet available to the authors of the earlier papers. The former method, called Diffusion Entropy (DE), was developed by the authors of Refs.[4, 5, 6] for the purpose of defining the asymptotic properties generated by the long-range correlation. When this method is applied to DNA sequences, it affords global information, this being unambiguous only in the ideal stationary case. The DNA sequences are non stationary and the adoption of the DE method must be supplemented by a non-stationarity indicator. This important indicator has been proposed in Ref. [7]. We refer to it as Non-Stationarity Entropic Index (NSEI) method. This is so because, as we shall see, this method is entropic in nature, it vanishes in the stationary case, and it is larger the larger the strength of non-stationarity. The measurement of long-range correlation is a delicate issue. The detection of non-stationarity is another delicate issue. The NSEI method addresses properly an even more delicate issue, this being the non-stationary character of long-range correlation.

With the use of these two brand new techniques we prove that moving from coding to non-coding and from eukaryotes to prokaryotes both the non-stationarity degree and the amount of long-range correlation increase. The deviations from stationarity and randomness are a sign of the role played by selection during the process of life evolution. The same argument applies to the increasing amount of non-stationarity, since this phenomenon is thought to be associated with the selection-induced increasing variety of molecular functions.

To make more solid this important biological conclusion we proceed as follows. We take into proper account the ideas that have been developed in the last few years to properly model the origin and the functions of the constraints on the DNA sequences randomness [8]. More specifically, we shed light into this issue by analyzing in the light of life evolution some key Low-Complexity Sequences (LCS). These LCS are defined as sequences containing only AT (homo-weak) or GC (homo-strong), or purines (GA), or pyrimidines (CT). The reason for choosing these particular non-random sequences lies in the fact that their presence is known to affect the DNA local conformational landscape, giving rise to non-B structures (the B structure is the usual double helix), and/or affecting the degree of bending, curving, twisting and rolling of DNA molecules. Conformational features are known to be true 3-dimensional codes for the interaction of DNA with proteins, a necessary condition for its involvement in chromosome organization and in the key functions of transcription and replication [9].

The outline of the paper is as follows: In section IA we describe some basic properties of LCS distributions and their influence on DNA structure. In section II we describe the global analysis through the DE of different genomes and compare it with LCS distribution data, while in section III we illustrate the NSEI method. Section IV aims at

showing the results of two methods at work, namely, the NSEI and a neural network trained by means of LCS lengths to distinguish between coding and non-coding sequences. Finally Section V is devoted to drawing some conclusions.

A. Distribution of LCS and their putative functional meaning

Provata and Almirantis [10] analyzed the size distribution of purine and pyrimidine clusters and found that coding and non-coding sequences yield an exponential decay and a power law decay, respectively. We also note that in eukaryotes the coding sequences relative amount is very low, whereas it is the largely dominant fraction of prokaryotes genomes. Both properties suggest to make an analysis of LCS length distributions in species placed in different positions in the “tree of life” [9]. In a preliminary paper [11] an algorithm was used to evaluate the LCS density in a large number of bacterial, archaeal and eukaryotic genomes. A clear difference was observed in the distributions of LCS relative amount between coding and non-coding regions and between prokaryotes and eukaryotes. In all genomes non-coding and Eukaryote sequences show the highest amount of LCS. To understand whether high-density values were accompanied by a random dispersion or by the presence of long LCS stretches, we decided to carry out an analysis of LCS length distributions. Herein the attention is centered on LCS known to give rise to non-B DNA conformations and to be involved in the control of gene expression and recombination, namely the homo-weak and the homo-strong. In the case of AT-rich (homo-weak) sequences we found higher values of LCS lengths in non-coding sequences vs. coding sequences and in eukariotes vs. Prokaryotes.

Fig. 1 shows this property for homo-weak noncoding sequences in some genomes, representative of archaea (M. Jannaschii), prokaryotes (B. Subtilis), unicellular eukaryotes (S. Cerevisiae) and multicellular eukaryotes (H. Sapiens, Chromosome I). We see an increasingly larger deviation from a single exponential distribution going from prokaryotes to more complex organisms with a larger amount of non-coding sequences. This property is less trivial than it may appear, since it is true also for GC-rich (homo-strong) sequences, as denoted by the curves with white symbols in Fig. 1. All these curves show a clear deviation from Poissonian behavior, even if their inverse-power-law decay has a large negative exponent (about -5). However, for all genomes, the curves for homo-weak LCS have a larger cut-off value than the corresponding ones for homo-strong LCS. This fact is indicative of a selection pressure against the lengthening of homo-strong sequence possibly to be attributed to their rigidity and conformation landscapes different from those of long AT-rich tracts. This leads us to choose homo-weak occurrence as a marker in the correlation analysis, as it will be explained below. Indeed, the presence of a decay slower than Poissonian suggests the possibility that correlation with an extend long range can be triggered by the presence of homo-weak and homo-strong LCS.

Remarkably, the authors of [12] performed a thorough study of intra and inter specific variability in upstream and coding sequences of a series of key genes in *Lycopersicum* (tomato) (the gene for ACC synthase), *Nicotiana* (the gene for Phytochrome), Primate species (the genes EMX and OTX 2 involved in brain development). All data showed a far higher variability in non-coding than in coding sequences, preferentially localized in LCS. In other words, different varieties have different lengths of AT-rich segments in the non-coding region before the gene. Quantitative RT-PCR data (Reverse Transcription-Polymerase Chain Reaction), a method to establish the amount of messenger-RNA, showed a clear variation of gene expression corresponding to different lengths of the homo-weak sequences.

Remarkably, the authors of [12] performed a thorough study of intra and inter-specific variability in ACC-synthase upstream sequences. They studied ACC-synthase upstream sequence in *Nicotiana* spp phytochrome regulatory sequences and in the same regions for the primates genes EMX-2, OTX-2. The results clearly showed that these LCS tend to be hyper-variables, i.e. they show a mutation frequency significantly higher than other DNA stretches, moving from and individual to another of the same species as well as from species to species, coherently with the aforementioned data on recombination. The interesting conclusion is that the three-dimensional code regulating the gene expression may be associated to a strongly *dynamical* DNA structure, with statistical constraints. This structure is probably associated to a process with long-range correlation. In the following section we shall analyze the long-range correlation present in the genome sequences and the relation between this property and the presence of LCS.

II. THE DIFFUSION ENTROPY METHOD APPLIED TO HOMOGENEOUS SEQUENCES

A. Global Diffusion Entropy

In recent papers [4, 5, 6] a new way of revealing long-range correlation, based on the detection of anomalous scaling has been proposed. In short, one defines a “marker” on a time sequences, and evaluates the probability $p(x; t)$ of having the number x of markers in a window of length t . The evaluation of $p(x; t)$ is done by moving a window of length t along the sequences and counting how many times one finds x markers inside this window. At this stage $p(x; t)$ is obtained by dividing this number by the total number of windows of size t , which is obviously $N - t + 1$,

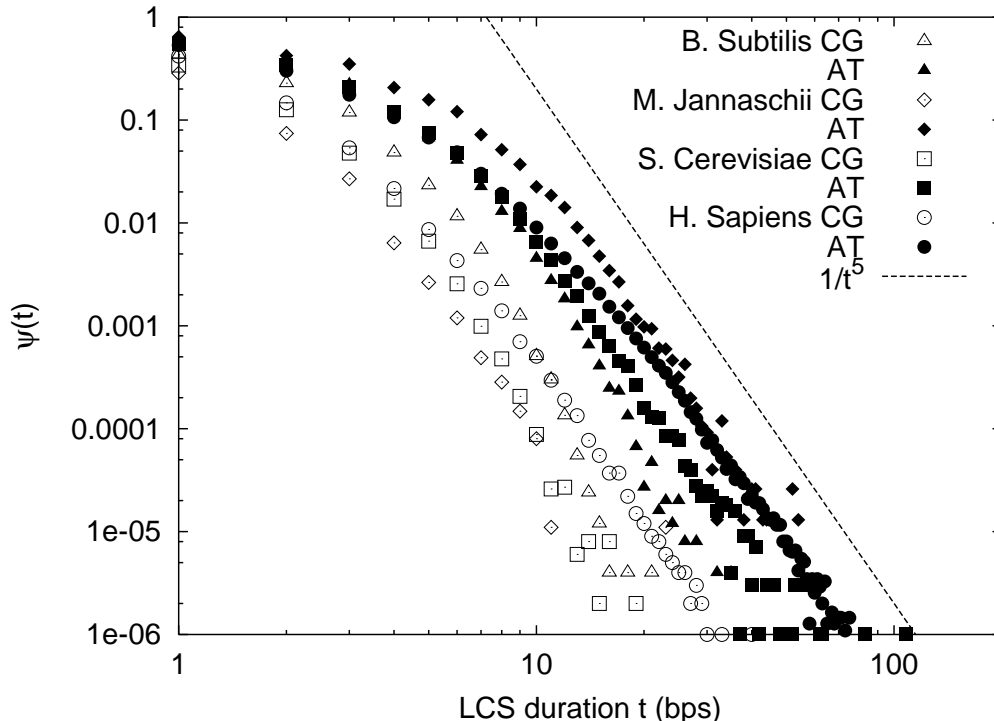


FIG. 1: Probability distribution of lengths of homo-weak (black symbols) and homo-strong (white symbols) non-coding sequences. Notice that the length distributions of homo-weak have a larger cutoff value; among these, cutoff values are larger for eukaryotes, namely for *S. Cerevisiae* (squares) and *H. Sapiens* (circles), than for archaea *M. Jannaschii* (diamonds) and bacterium *B. Subtilis* (triangles). Dotted line represents an eye-guide decay $\propto t^{-5}$.

where N is the total length of the sequence. In the case of large values of x and t , the continuous approximation is legitimate, and, in the ergodic and stationary condition, a scaling relation is expected, namely In case of large values of x and t , the continuous approximation is legitimate, and, in the ergodic and stationary condition, we expect scaling, namely, we expect

$$p(x; t) = \frac{1}{t^\delta} F\left(\frac{x}{t^\delta}\right), \quad (1)$$

where δ is said to be the *scaling index* and F is a function, sometimes called “master curve”. If F is the Gauss function, δ is the known Hurst index, and if the further condition $\delta = 0.5$ is obeyed, then the process is said to be Poissonian, namely there is no long-range memory regulating the occurrence of markers in time. It is straightforward to show that the Shannon Information

$$S(t) = \int_{-\infty}^{\infty} dx p(x; t) \ln p(x; t) \quad (2)$$

with condition (1) leads to

$$S(t) = k + \delta \ln t, \quad (3)$$

where k is a constant. A linear fit of $S(t)$ in log-normal paper allows an estimation of δ .

B. The CMM model of DNA

In recent years many groups have agreed to consider DNA sequences as a mixture of long- and short- range correlation, the latter blurring the strength of the former. A simple model, originally proposed by Araujo et al.

[13], and later adopted independently by the authors of Refs. [14], [15] and [16], to name a few, is the Copying Mistakes Map (CMM)[14]. This is the superposition of two models, one consisting of a pure random choice, and the other of an intermittent generator of homogenous sequences, yielding long-range correlation. Both models provide a sequence, where the i -th nucleotide of the resulting DNA sequence is taken from the first component (the white one) with probability $1 - \epsilon$ and from the second with probability ϵ . The resulting correlation function is proven [14] to be

$$C(t) = \delta_{i,0} + \epsilon^2 \left(\frac{T}{T+t} \right)^\beta, \quad (4)$$

where $\delta_{i,j}$ is the Kroeneker delta, while T and β are two positive parameters of the intermittent model. Long-range memory is normally characterized by the condition $\beta < 1$, which makes the correlation function (4) not integrable.

As shown in ref. [14], the second moment and the Hurst analysis reveal a short-time behavior which is dominated by the random component, while the correlated part dominates in the long-time limit. By the same token, DE method applied to CMM sequences, yields for $S(t)$ a curve that starts with a slope of $\delta = 0.5$, and then after a knee, tends asymptotically to higher value of δ corresponding to the Lévy scaling $\delta = 1/(\beta + 1)$. This behavior, as reported in Ref. [17], is illustrated in fig.2, which shows that the position of the knee is a monotonic function with respect to ϵ : the larger ϵ the smaller the position of the knee.

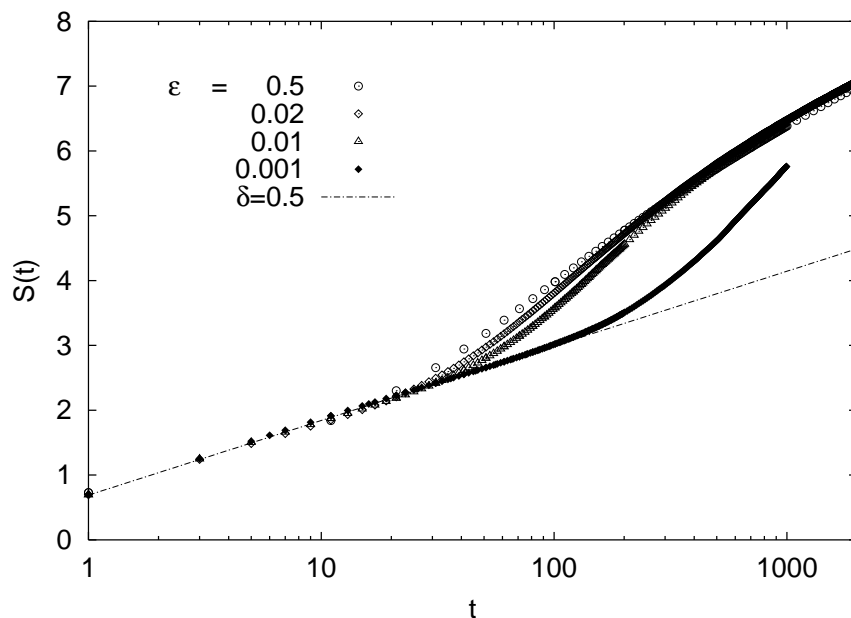


FIG. 2: Diffusion Entropy for CMM's with the same δ , and various values of ϵ .

C. DE at work on real genomes

As earlier shown, the DE method establishes the values of two quantities: the ratio of the correlated to the uncorrelated component intensity of the CMM model (through the position of the knee) and the anomalous scaling index δ . As an example, we show in fig. 3 the DE analysis on the chromosome IV of *Saccharomices Cerevisiae*. In Tab.I we report the results corresponding to different genomes grouped according to whether they are bacteria, archaea or eukaryotes. All these analyses were performed using as marker the homo-weak occurrence in the series. This means that we put 1 at position i if the i -th nucleotide *and* the previous one are weak bases (AT), and 0 elsewhere. This choice was suggested by the non-exponential decay in the length distribution of homo-weak sequences shown in fig.1a. We made the hypothesis that this non-exponential behavior can be connected with the long-range correlation observed in the genomes.

Tab.I shows two interesting results: the former is that the value of δ does not seem to depend on the position in the evolutionary tree. The latter is that the position of the knee seems to change with moving from bacteria to archaea and eukaryotes. As shown in the table, the weight of the correlated component in bacteria is larger than

Genomes	knee ± 5	$\delta \pm .04$
Bacteria		
M. pneumoniae *	80	0.76
T. maritima *	90	0.75
R. prowazekii *	90	0.60
H. influenzae *	60	0.71
B. subtilis *	100	0.78
E. coli *	100	0.73
A. aeolicus *	90	0.72
Synechocystis Sp. *	80	0.73
Archaea		
M. thermoautotrophycum *	60	0.76
A. fulgidus *	60	0.68
M. jannaschii *	40	0.68
P. abyssi *	100	0.76
Eukaryotes		
S. cerevisiae *	50	0.70
H. sapiens Chr. 1 *	20	0.88
C. elegans *	5	0.76
A. thaliana *	15	0.75

TABLE I: The * denotes complete genomes or chromosomes. The analysis was performed using the homo-weak occurrence as a marker.

in eukaryotes, archaea being somewhat intermediate between bacteria and eukaryotes. It is also worth noticing that within eukaryotes, the unicellular, almost intronless, *S. Cerevisiae* has the largest knee value.

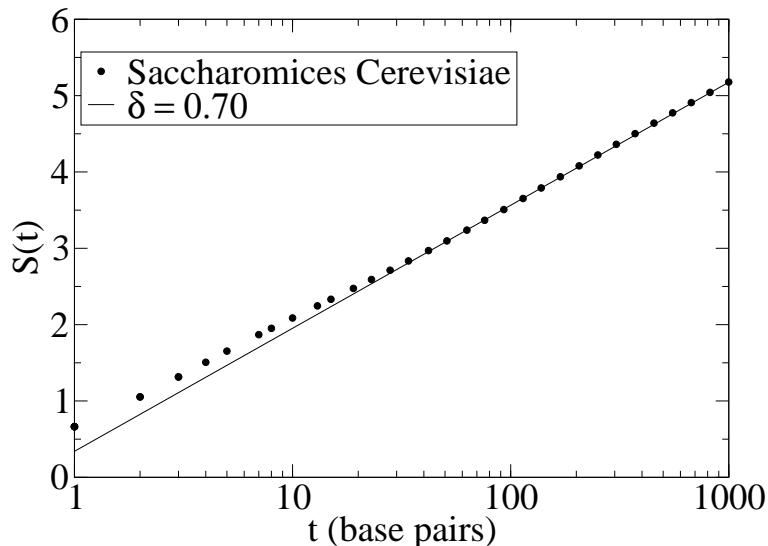


FIG. 3: Diffusion Entropy analysis for *Saccharomices Cerevisiae*.

III. THE NON-STATIONARITY ENTROPIC INDEX

In order to study the local properties of DNA sequences with special focus on the distribution and variability of homogeneous sequences, we use a new method, the NSEI method. This method is derived from the DE method [7] as an earlier method, called CASSANDRA algorithm [7, 18]. The DE method affords global information, while both CASSANDRA and NSEI method aim at affording local information. The CASSANDRA method measures the

rate of transition from dynamics to thermodynamics through comparison with ordinary Brownian motion. The NSEI method focuses on the local deviation from the stationary behavior. The first step of the NSEI method is to build the diffusion entropy function $S(t)$ for each window of size L with $L \gg t$, thought of a complete sequence. In this way we obtain several functions $S_j(t)$, where the subscript j refers to the portion of the sequence used to calculate $S_j(t)$. Formally, we write

$$x_j(t, l) \equiv \sum_{i=j+l}^{j+l+t} \xi_i, \text{ with } 0 < l < L - t \quad (5)$$

where ξ_i is the DNA sequences after marking the homogeneous sequences, as earlier illustrated, and j and L denote the beginning and the length of the big window, respectively. We assign to the integers j multiple values of a given integer J , namely $j = 0, J, 2J, \dots$, thus avoiding too large overlaps between two windows of length L , corresponding to two consecutive choices of j . At fixed t and L we obtain for different l a probability distribution $p_j(x, t)$. Calculating the entropy of this distribution, we obtain

$$S_j(t) \equiv \int dx p_j(x, t) \log p_j(x, t) \quad (6)$$

Now we are ready to define the non-stationarity index, indicated as Ξ_j , as follows

$$\Xi_j = \int_0^t dt' (S_j(t') - \bar{S}_j(t')) \quad (7)$$

where

$$\bar{S}_j(t) \equiv \frac{1}{m} \sum_{i=j-m-1}^{j-1} S_i(t) \quad (8)$$

Note that m is the number of windows involved by the average process of Eq.(8). Depending on the step J by which j increases we obtain that the comparison between local and previous diffusion behavior involves $m \cdot J$ points of the sequence. Note that if the sequence is perfectly stationary we have $\Xi_j = 0$, otherwise we have a value different from zero.

IV. DNA FUNCTION AND LOCAL CORRELATION

In Section IA we saw that non-coding sequences contain a number of homogeneous sequences larger than coding sequences. Experimental evidence shows that LCS tend to occur either in the upstream region of each gene, i.e. immediately before the occurrence of a gene, or in introns. It is also known that both upstream sequences and, to a lesser extent, introns, are the regions endowed with regulatory roles in which LCS are involved. In this section we evaluate the change of local correlation, according to the NSEI method, and we see that this change is often associated with the beginning of a coding portion. Thus, using biological consideration, we are led to establish a plausible link between the change of DNA sequence correlation and the functional change of the sequence. In other words, we expect that the boundary between a coding and a non-coding segment is revealed by either a positive or negative peak of the NSEI index, as a function of the position j along the sequence. In Fig. 4 we show an example where this hypothesis is verified to a satisfactory extent. As earlier stated, the analysis was carried out using as marker the occurrence of homo-weak sequences. Peak recognition has been realized in the following way. The data have been smoothed through a moving linear interpolation with ten points. The maximum indexes were identified looking at the “derivative” thus obtained; only maximum indices with a value larger than the standard deviation, calculated over the whole signal, were selected.

The NSEI method should reveal the beginning and the end of a LCS with peaks. It is important to point out that the NSEI method, although being the most convenient indicator of non-stationarity, within the theoretical framework of DE method, does not have a perfect efficiency. This means that the NSEI signals correctly the existence of a boundary between two distinct regions. This is a true positive, denoted by the symbol TP . There are cases, however, when the NSEI signals a boundary that does not exist. This is called a false positive, and it is denoted by the symbol FP . By the same token we denote by TN and FN , the true and false case, respectively, of a missing boundary. The

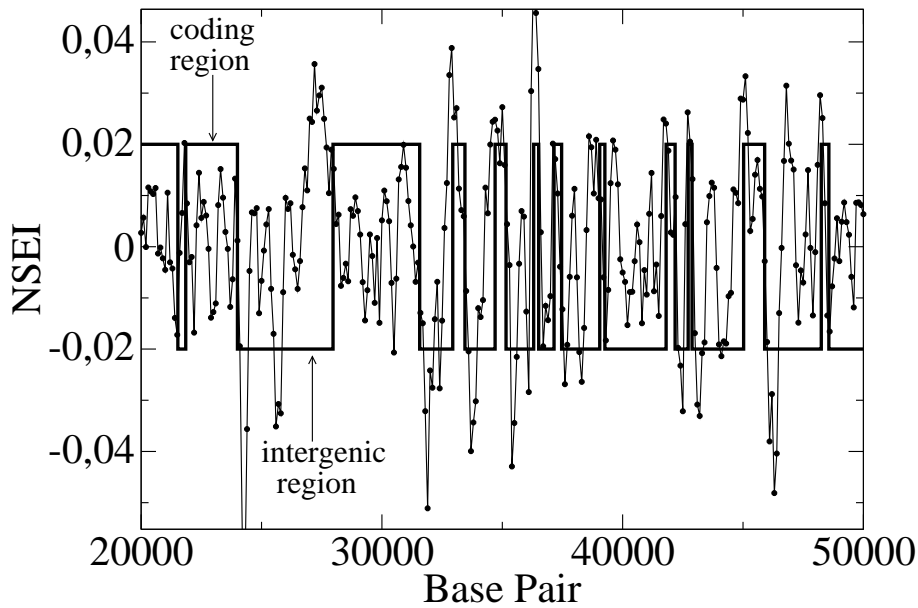


FIG. 4: Non-Stationarity Entropic Index for *Saccharomyces Cerevisiae*. The abscissa axis denote the position of center of the large window with length $L = 400$. Other parameters of the analysis are: the jump size $J = 100$, the number of averaged windows $m = 4$ and maximum time $t = 12$ for entropy evaluation. The thick line denotes the displacements of coding and noncoding portion of the genome,

total number of borders is given by $FN + TP$, while the total number of cases signaled by the NSEI, true or false, is given by $TP + FP$. It is worth noticing that the observed peaks, in addition to corresponding to true peaks, must be found in position close enough to the position of the real borders, namely at a distance smaller than a critical value T , which is of the same order as L .

We are now in the proper position to establish the accuracy of the NSEI. We can judge this method satisfactory if we prove that it affords a number of correct guesses significantly larger than the random choice. To assess this issue we apply to the NSEI method a technique of assessment frequently used in Information Extraction [19]. We define two quantities, Precision and Recall. Precision P is a measure of how accurately the displacements of coding/non-coding boundaries are guessed, while Recall R is a measure of how many of these regions are correctly located. Formally, we write

$$P = \frac{TP}{TP + FP} \quad (9)$$

and

$$R = \frac{TP}{TP + FN} \quad (10)$$

We compare the P and R of our predictor to a baseline score associated with $TP + FP$ random choices for the position of the boundaries. The “true” classification was done according to documents accompanying DNA sequences in Genbank database, regardless whether the annotation was experimental or putative. Although this makes our esteem of P and R questionable, we think that the improvement with respect to the random baseline will not diminished after a more accurate experimental annotation. Results are summarized in table II. As shown in the table, the NSEI method reveals statistically significant improvement with respect to the baseline, especially for eukaryotes, where the marker adopted (homo-weak) has a larger biological significance.

We end this section by reporting results stemming from a completely different way of detecting coding and non-coding sequences. This alternative way confirms the correlation between the changes of the amount of LCS and entropy changes, when moving from the coding to the non coding regions. A three layer feed forward neural network was built and trained on homogeneous sequences (homo AT; homo GC; homopurine; homopyrimidine) [20]. The network involves eight neurons in the input layer, four in the intermediate, one in the output one. The network has been trained on 100 tracks each of 300 nucleotides of known coding and on 100 for known non coding regions. Inputs

Genome	$TP + FP$	TP	FP	$TP + FN$	P	R	Random P	Random R
A. aeolicus	1089	457	632	1744	0.420	0.262	0.278	0.173
A. fulgidus	1497	879	618	2992	0.587	0.294	0.326	0.163
B. subtilis	3157	1673	1484	7584	0.530	0.221	0.424	0.177
B. burgdorferi	627	237	390	1252	0.378	0.189	0.314	0.157
C. tetani	2517	1236	1281	6556	0.491	0.189	0.426	0.163
V. cholerae	2898	1631	1267	6166	0.563	0.265	0.381	0.179
E.coli	3235	1966	1269	6894	0.608	0.285	0.387	0.181
H. influenzae	1215	619	596	2920	0.509	0.212	0.401	0.167
H. pylorii	1143	551	592	2406	0.482	0.229	0.349	0.166
M. pneumoniae	504	241	263	926	0.478	0.260	0.313	0.170
N. gonorrhoeae	1607	1065	542	3668	0.663	0.290	0.428	0.187
P. aeruginosa	4037	2796	1241	9310	0.693	0.300	0.381	0.165
P. abyssi	1216	638	578	2302	0.525	0.277	0.323	0.170
R. prowazekii	762	301	461	1439	0.395	0.209	0.372	0.197
S. typhi	3312	1984	1328	7260	0.599	0.273	0.390	0.178
Synechococcus spp.	2464	1415	1049	5729	0.574	0.247	0.425	0.183
T. maritima	1309	550	759	2154	0.420	0.255	0.264	0.160
D. radiodurans	2169	1302	867	4531	0.600	0.287	0.376	0.180
M. Jannaschii	1088	578	510	2858	0.531	0.202	0.424	0.161
M. thermoautotrophicum	1305	893	412	3014	0.684	0.296	0.407	0.176
S. cerevisiae	6733	4096	2637	10506	0.608	0.390	0.337	0.216
A. thaliana	7698	2203	5495	4201	0.286	0.524	0.137	0.251
H. sapiens Chr1	7413	86	7327	208	0.012	0.413	0.007	0.242
D. melanogaster	7430	1901	5529	2577	0.256	0.738	0.083	0.239
C. elegans	7007	1175	5832	4119	0.168	0.285	0.131	0.223

TABLE II: The parameters for the analysis reported herein are: large windows with length $L = 400$, jump size $J = 100$, number of averaged windows $m = 4$ and $t = 12$ for maximum time of entropy evaluation. Different boxes divide species into four groups: bacteria, archaea, unicellular and multicellular eukaryotes.

Genome	N_{tot}	TP	ncp	TN	ncn	Q	W
A. aeolicus	900	477	110	658	97	0.767	0.678
M. Jannaschii	900	730	46	531	95	0.727	0.811
S. cerevisiae (chr 1)	900	566	79	813	40	0.923	0.761
S. cerevisiae (chr 10)	900	651	45	700	41	0.804	0.774
A. thaliana (chr 1)	900	702	20	773	26	0.874	0.813
C. elegans (chr 1)	900	853	5	846	7	0.948	0.953
D. melanogaster	900	627	17	889	6	0.992	0.776

TABLE III: The parameters for the analysis reported herein are: TP =true positive non coding tracks, TN =true positive coding tracks, ncp = non classified non coding tracks, ncn = non classified coding tracks, FP = coding tracks classified as non coding, FN = non coding tracks classified as coding, $Q = TP/(TP + FP)$ and $W = TN/(TN + FN)$. Different boxes divide bacteria, yeasts and multicellular eukaryotes.

of the network are 1) percentage of the sequence covered by homogeneous tracks 2) average length of homogeneous tracks in the observed sequence. Then 900 tracks have been screened with the trained network for each class. This operation has been performed for each species listed in the table III. The precision level of annotation (identification of the two classes) is very high as seen from Q and W values. For true positives (Q), moreover, eukaryotes seem to perform better than prokaryotes, coherently with the higher non-coding/coding ratio.

It is worth noticing that this second way of detecting the change of the DNA function is complementary to the first one. Indeed the NSEI method, which does not require any form of training, yields a model-oriented location of the function change on a scale comparable with L . On the other hand the neural network technique is more precise and can become very efficient when performed on the basis of evidence obtained by means with NSEI.

V. CONCLUSIONS

In this paper we discussed how to derive a coherent picture from the study of LCS, local properties, and long-range correlation, global properties. Thanks to the DE technique we showed that long-range correlation seems to have a quite homogeneous behavior when looked at using a large scale. Variations in the transient behavior, however, confirm an increase of the non-random component with moving from bacteria to archaea, from archaea to the unicellular eukaryote *S. cerevisiae*, and from this to multi-cellular plants and animals. This increase throughout the evolution scale is consistent with that of non-coding sequences, which are known to cover less than 10% of prokaryotes genomes and well over 90% of the eukaryotes ones. A plausible hypothesis, to explain these properties in terms of function, is that non-coding sequences can be more freely “filled” with “hidden codes”. These hidden codes are mainly used for the recognition of protein molecules, necessary for the organization and function of the DNA sequence and other ligands. Remarkably, these codes, and in general non-coding sequences as well, tend to be hyper-variable, due to the presence of LCS, suggesting *a positive role of mutational noise in regulatory sequences* (see Ref [9] for a through discussion).

To afford some more details on why to connect LCS, conformational landscapes, regulation and structure of genomes, we should note that some constraints may play a role in eukaryotes for DNA “packaging” in nucleosomes and chromosomes. Moreover, it is well known that DNA activation for transcription and replication is due to the recognition by proteins of DNA regions, and vice-versa, based on complementary conformations leading to formation of complexes. Protein-DNA complexes involve at the same time a high number of molecules where interaction needs a specific global organization favored by DNA curving, bending, twisting and rolling at the right points. This may require the presence of non-random tracts with the needed conformational landscape. The strategy reported herein, namely the adoption of NSEI and of neural networks, fulfills the biologist’s need for research leading to the characterization of the living state of matter (LSM) [22] on one hand, to the identification of specific functional sequences in sequenced genomes on the other.

We investigated on the connection between correlation and LCS, and between LCS and the regulation of a gene transcription. We showed that the variation in the statistics of homo-weak sequences, i.e. a particular kind of LCS, yielding specific DNA conformational landscapes, strongly correlates with changes in DNA function and, especially, that these sequences signal the beginning of a coding region. We studied these variations with the help of the NSEI algorithm obtaining satisfactory results. The accuracy achieved, although affording significant information, is not high, in comparison with other annotation methods currently used by molecular biologists. In fact, with some of these methods, the percentage of failure is now around 10%-15%. Better results were herein obtained with a neural network trained on LCS, the class of non-random sequences. The NSEI method, however, a model-based technique, affords a way to scan the whole genome, in the search for non-stationary segments, where a transition from a given degree of correlation to another occurs: The putative boundaries between coding and non-coding DNA may generate the segmented input tracks for the neural network, a method with a larger accuracy for the final categorization. The NSEI method is based on a DNA dynamic model, compatible with the DE method, which signals the long-range correlation of the sequence. If the correlation strength undergoes local changes, these are signaled by the NSEI method. Moreover, the increase in complexity in the “tree of life” correlates with an increase in non-coding DNA and in the number of coding/non-coding boundaries. A high precision on the same task of recognizing coding sequences has been obtained by other authors with algorithms based on specific motifs known to be present in non-coding regions or exploiting existing periodicities [21]. Probably an even higher precision could be obtained through the combination of all methods. It is therefore quite important that the NSEI results were obtained without using all these properties but only the variation in the statistics of homo-weak sequences.

A reasonable interpretation of these data all taken together, could be that several kinds of functionally constrained sequences have been fixed in genomes throughout evolution and that average higher correlation values in non-coding sequences are a result of this process. However at a local level, while to some extent LCS can be present also in coding regions, precise annotation (distinction between coding and non-coding sequences) has to rely on the detection of constraints (codes) specific for each class of DNA regions. For instance, while a 3-periodical behavior, in phase with the triplet “universal” code is typical of coding regions [14, 21], specific motifs and rather long LCS have been shown to be distinctive of non-coding regions, which are free from coding constraints [14]. In other words, the relatively low level of constraints corresponding to long-range correlations (and to the presence of LCS) in transcribed and translated sequences can be attributed to the fact that in that case selection has not been acting on DNA, but on proteins, and there is not a direct relationship between constraints in the two classes of molecules.

As a final remark, looking at LCS, we point out an almost paradoxical result, namely that hypervariable sequences carry a constraint. LCS hypervariability is known to be favored in regions of genes where variation, leading to protein variability, is essential. For instance, it can be useful for the right response to hypervariable pathogens. Lower complexity levels in eukaryotes seem therefore to derive from a wide series of constraints ranging from periodicities to different kinds of short-range and long-range correlations and to the presence of LCS of varying length. This

hypothesis is supported by the present work, suggesting the NSEI as a tool for analyzing data, when looking at this kind of constraints, because of its locality and its wise use of statistics. Furthermore, we want to point out that the NSEI emerges from the theoretical background of Ref. [7]. The DE method was originally introduced as an efficient technique to evaluate scaling, this being a global property, implying stationary condition. The NSEI is the best way, known to us in this moment, to address the challenging issue of non-stationarity from the same dynamic approach to complexity as that behind the foundation itself of the DE method. From a conceptual point of view, more than from an application point of view, we want to stress that this technique of analysis, resting on entropy formalism, might have the important role of helping the foundation of the LSM theory [22, 23]. As explained in Ref. [22], in fact, the relation between hyper-variable sequences and regulation is a key aspect of the LSM perspective, and the investigation of this issue based on the NSEI might make easier for the advocates of the LSM perspective to express the main ideas of this theoretical proposal with the language of statistical mechanics, probably anomalous statistical mechanics.

Acknowledgments PG gratefully acknowledges financial support from ARO through Grant DAAD19-02-0037

-
- [1] Li, W. and Kaneko, K. 1992. Long-range correlation and partial 1/f spectrum in a noncoding DNA sequence. *Europhys. Lett.*, **17**, 655–660.
 - [2] R. Voss. Evolution of long-range fractal correlations and 1/f noise in DNA base sequences. *Phys. Rev. Letters*, **68**:3805–3808, 1992.
 - [3] C. -K. Peng, S. V. Buldyrev, S. Havlin, M. Simons, H. E. Stanley, and A. L. Goldberger, *Phys. Rev. E*, **49**, 1685 (1994); C. -K. Peng, S. Havlin, H. E. Stanley, and A. L. Goldberger, *Chaos*, **5**, 82 (1995);
 - [4] P. Grigolini, L. Palatella, G. Raffaelli, Asymmetric Anomalous Diffusion, an Efficient Way to Detect Memory in Time Series, *Fractals* **9**, 439-449 (2001).
 - [5] Nicola Scafetta, Patti Hamilton and Paolo Grigolini, The Thermodynamics of Social Process: the Teen Birth Phenomenon, *Fractals*, **9**, 193 (2001); Nicola Scafetta, and Paolo Grigolini, Scaling detection in time series: diffusion entropy analysis, *Phys. Rev. E* **66**, 036130 (2002)
 - [6] P. Allegrini, P. Grigolini, P. Hamilton, L. Palatella, G. Raffaelli, Memory beyond Memory in Heart Beating, a Sign of Healthy Physiological Condition *Phys. Rev. E* **65**, 041926 (2002).
 - [7] P. Allegrini, V. Benci, P. Grigolini, P. Hamilton, M. Ignaccolo, G. Menconi, L. Palatella, G. Raffaelli, N. Scafetta, M. Virgilio, J. Yang, Compression and Diffusion: a Joint Approach to Detect Complexity, *Chaos Solitons & Fractals* **15**, 517-535 (2003).
 - [8] P. Lió, S. Ruffo, M. Buiatti, Third Codon G + C Periodicity as a Possible Signal for an "Internal" Selective Constraint, *Journal of Theoretical Biology*, **171**(2),215-223 (Nov 21, 1994).
 - [9] M. Buiatti, P. Bogani, C. Acquisti, G. Mersi, L. Fronzoni, The living state of matter between noise and homeorretic constraints, in the forthcoming volume *Interdisciplinary applications of ideas from nonextensive statistical mechanics and thermodynamics* ed. by Murray Gell-Mann and Constantino Tsallis, Oxford University Press, Oxford (2003).
 - [10] A. Provata and Y. Almirantis, Scaling properties of coding and non-coding DNA sequences, *Phys. A*, v. 247 p.p. 482 (1997).
 - [11] M. Buiatti, C. Acquisti, G. Mersi, P. Bogani, The biological meaning of DNA correlations, in *Biology and Medicine*, G. Losa, Birkhauser, Basel p. 235 (2002).
 - [12] Bogani, P., Simoni, A., Lió, P., Germinario, A., Buiatti, M. (2001). Molecular variation in plant cell populations evolving in vitro in different physiological contexts. *Genome*, **44**:1-10; Bogani P., Scialpi, A., Masieri M., Nardi M., Rosati A., Gori M., Buiatti M. (2003). Functional markers for the study of genetic variation in tomato. *Proc. 7th Int. Con. Plant. Mol. Biol.*, in press.
 - [13] S.V. Buldyrev, A.L. Goldberger, S. Havlin, C.-K. Peng, M. Simons and H.E. Stanley , Generalized Lévy walk model for DNA nucleotide sequences. *Phys. Rev. E* **47** (1993), pp. 4514-4523
 - [14] P. Allegrini, M. Barbi, P. Grigolini and B. J. West, Dynamical model for DNA sequences, *Phys. Rev. E*, v. 52, p. 5281 (1995).
 - [15] P. Allegrini, M. Buiatti, P. Grigolini and B. J. West, Non-Gaussian statistics of anomalous diffusion: The DNA sequences of prokaryotes, *Phys. Rev. E*, v. 58, p. 3640 (1998).
 - [16] D. E. Strier, D. H. Zanette, Self similarity in a model of genetic microevolution, *Physica A*, Volume 257, 1998, Pages 530-535
 - [17] Nicola Scafetta, Vito Latora and Paolo Grigolini, Lévy statistics in coding and non-coding nucleotide sequences, *Physics Letters A* **299** (5-6), 565-570 (2002); Nicola Scafetta, Vito Latora and Paolo Grigolini, Scaling without detrending: the diffusion entropy method applied to the DNA sequences, *Phys. Rev. E* **66**, 031906 (2002).
 - [18] P. Allegrini, P. Grigolini, L. Palatella, G. Raffaelli, M. Virgilio, Facing non-stationarity Conditions with a New Indicator of Entropy Increase: the CASSANDRA Algorithm, in: Novak, M.N. (ed.): *Emergent Nature*. World Scientific, Singapore (2002) 173-184.
 - [19] See, for instance, K.S. Jones. *Information Retrieval Experiment*. Butterworth and Co., 1981.
 - [20] D. Graupel, *Principle of Artificial Neural Networks*, World Scientific, Singapore (1997).

- [21] I. Grosse, H. Herzel, S.V. Buldyrev, H.E. Stanley , Species independent of mutual information in coding and noncoding DNA, Phys. Rev. E, v. 61, p. p. 5624 (2000).
- [22] M. Buiatti, N. Buiatti, Towards characterization of the living state od matter, Chaos, Solitons and Fractals, these Proceedings.
- [23] P. Allegrini, G. Aquino, P. Grigolini, L. Palatella, A. Rosa, *Breakdown of the Onsager Principle as a Sign of Aging*, submitted to Phys. Rev. E.